ACS APPLIED MATERIALS & INTERFACES

Research Article

www.acsami.org

One-Step Generation of Engineered Drug-Laden Poly(lactic-*co*-glycolic acid) Micropatterned with Teflon Chips for Potential Application in Tendon Restoration

Xuetao Shi,*[,†] Yihua Zhao,[‡] Jianhua Zhou,[†,‡] Song Chen,[§] and Hongkai Wu*[,†,‡]

[†]WPI Advanced Institute for Materials Research, Tohoku University, 2-1-1 Katahira, Aoba-ku, Sendai, 980-8577, Japan

[‡]Department of Chemistry, Hong Kong University of Science and Technology, Hong Kong, China

[§]Biomaterials Unit, National Institute for Materials Science, Tsukuba 305-0047, Japan

ABSTRACT: Regulating cellular behaviors such as cellular spatial arrangement and cellular phenotype is critical for managing tissue microstructure and biological function for engineered tissue regeneration. We herein pattern drug-laden poly(lactic-*co*-glycolic acid) (PLGA) into grooves using novel Teflon stamps (that possess excellent properties of resistance to harsh organic solvents and molecular adsorption) for engineered tendon-repair therapeutics. The drug release and biological properties of melatonin-laden PLGA grooved micropatterns are investigated. The results reveal that fibroblasts cultured on the melatonin-laden PLGA groove micropatterns not only display significant cell alignment that mimics the cell behavior in native tendon, but also promote the secretion of a major extracellular matrix in tendon, type I collagen, indicating great potential for the engineering of functional tendon regeneration.

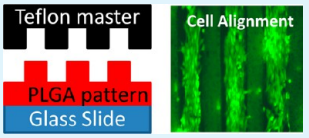

KEYWORDS: *poly(lactic-co-glycolic acid), micropatterning, Teflon, tendon, melatonin*

1. INTRODUCTION

Injuries to tendons are among the most common injuries in the physically active population.[1,2] Despite various strategies in current available therapies including autografts and allografts, there still remain numerous insurmountable challenges, including inferior functionalities of repaired tendons, limited source, and immunological rejection.[2−4] Currently, alternative therapies for tendon repair using tissue-engineering strategies have emerged.[5,6] Tendon tissue-engineering strategy represents a scientific and biomimetic approach that attempts to use well-designed cell-biomaterial composite to simulate the native structure and functions of tendon, and eventually induces tendon remolding.[1,6]

Elaborating cell spatial arrangement takes a crucial role in tissue microarchitecture and biological functions. For instance, in a native tendon, tendon fibers are constructed in an exquisite way by assembling of collagen fibers and cells in parallel arrays.[7] The unique mechanical properties involving the promotion of joint stability and the permission of body locomotion of tendon are mainly attributed to this exquisitely orientated assembly of cells and extracellular matrix.[1,8] Hence, to engineer a tendon using a biomimetic strategy, the micropatterning technique that can elaborate surfaces with arbitrary motifs using pre-prepared stamps becomes one of the advisable options.[9,10] By implementing the micropatterning technique, different topographical motifs can be printed on the surfaces of various materials including polymers, inorganic materials, and metals.[10−15] The generated micropatterns have been broadly used to manipulate cell behaviors including steering cell orientation and regulating cell differentiation, and even to construct tissues/organs due to their outstanding performances in inducing biological responses of cells by topographical cues.[16−19]

Besides cellular arrangement, cellular behavior can also be regulated by chemical/biological cues. For example, osteogenic factors including growth factors[20] and bisphosphate[21] induce or promote the osteogenesis of stem cells or osteoblasts. Cell adhesion peptide Arg-Gly-Asp (RGD) influences the viability, attachment, and differentiation of stem cells.[22] In this study, we intend to develop a micropatterned scaffold that combines the functions of managing cellular alignment and releasing functional molecules. Poly(lactic-*co*-glycolic acid) (PLGA), a synthesized copolymer with tunable biodegradable and low cytotoxicity properties, is one of the most popular biocompatible materials for biomedical devices and tissue-engineering applications.[23] PLGA has also displayed appealing features for encapsulating various therapeutic compounds and can be processed into diverse shapes such as fibers, microspheres and spongelike porous blocks.[24−30] In virtue of these superiorities, development of functionalized micropatterns using PLGA is an advisable choice.

Currently, PLGA micropatterns are generated by various routes including laser interference lithography and thermal-pressing micropatterning.[19] However, complicated procedures and expensive equipment are required for laser interference lithography. For thermal-pressing micropatterning, it is facile and convenient but a high temperature is required. If a drug/protein-laden PLGA micropattern is developed using this method, then the high temperature can severely influence the

Received: June 25, 2013
Accepted: October 10, 2013
Published: October 10, 2013

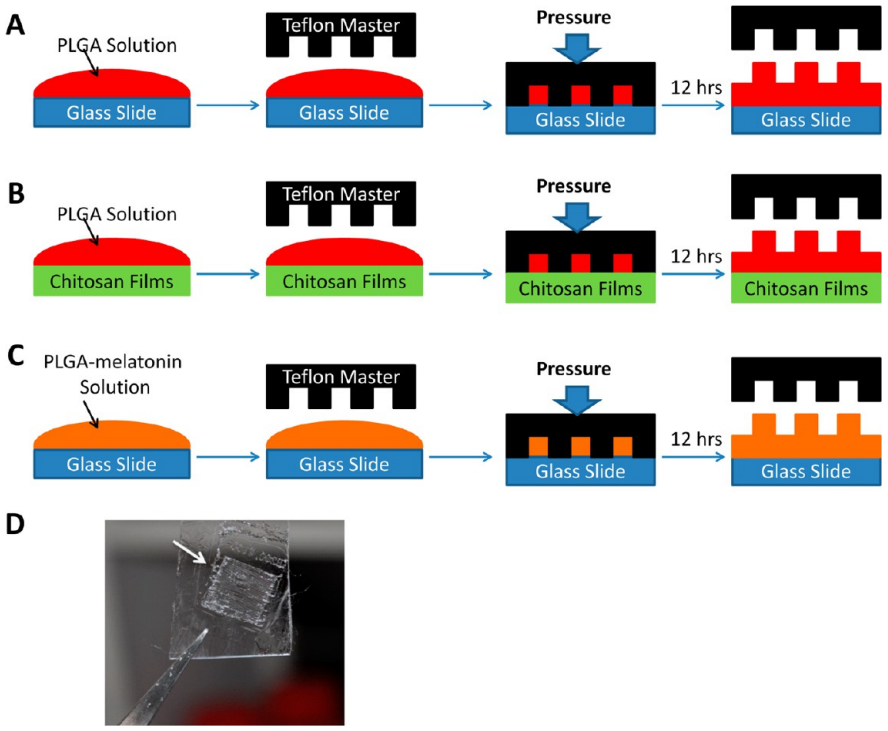

Figure 1. Schematics of the generation of PLGA micropatterns on a glass slide (A), PLGA micropatterns on a chitosan film (B), and melatonin-laden PLGA micropatterns (C) by Teflon stamps; and the morphology of generated PLGA micropatterns on a glass slide (D).

bioactivity and effects of drug/protein. To overcome these drawbacks, it is possible to pattern PLGA in its liquid phase (PLGA dissolved in methylene chloride) by soft lithography. However, the usage of prevalent polydimethysiloxane (PDMS) as stamps to create the microscopic features on PLGA (that can only be dissolved in harsh organic solvents) solution is still restricted.[31] Our approach to address this challenge is inspired by the unique characteristics of Teflon plastics. All Teflon plastics, a group of perfluorinated polymers invented by DuPont, are endowed with the fine characteristics of non-sticking or nonadsorbing for almost anything. Moreover, it shows strong resistance to almost all organic solvents including acetone, chloroform, and methylene chloride.[32] Because of these excellent properties, Teflon stamps would be an excellent candidate to generate micropatterns of PLGA in methylene chloride instead of conventional PDMS stamps.[32,33]

This work reports the generation of different PLGA micropatterns using Teflon stamps. We further develop drug-laden PLGA grooved micropatterns (PGMs) for the application in potential tendon restoration. Melatonin, a hormone secreted by the pineal gland in the brain, which can regulate collagen accumulation, is loaded into the PGMs.[34] The drug-release behavior, cell alignment, and cell biological properties are investigated. The simultaneous stimulation of both drug signal and topographical cue (grooved micropattern) may significantly promote tendon regeneration.

2. MATERIALS AND METHODS

2.1. Fabrication of Teflon Stamp. A thin PDMS (GE, China) master was molded from photoresist microstructures fabricated by standard photolithography, and then sealed to a glass slide. A Teflon plate (~1.0 mm thick, Yuyisong Inc., China) was put between the PDMS master and a flat glass slide. The sandwich assembly was placed on a hot compressor (TM-101F, Taiming, Inc.), embossed for 5 min at 275 °C, and then allowed to cool at room temperature. A Teflon stamp was obtained after removing the PDMS master and glass slide.[32,35−38]

2.2. Organic Solvent Resistance. Teflon and PDMS slides (approximately 1 cm × 1 cm) were incubated in 10 mL of methylene chloride. After 3 h, the slides were taken out and washed with deionized water for five times. The surface structure features of the slides were investigated by scanning electron microscopy (SEM, JIB-4600F).

2.3. Molecule Adsorption Test. Teflon and PDMS slides (approximately 1 cm × 1 cm) were incubated in 2% rhodamine solution and 2% fluoresceinisothiocyanato-dextran (FITC-Dex), respectively. After 3 h, the slides were taken out and washed with deionized water five times, and the molecules adsorbed on the surface of the slides were examined under a fluorescent microscope (Zeiss, Germany).

2.4. Fabrication of PLGA Micropatterns/Melatonin-Laden PLGA Micropatterns. PLGA micropatterns or melatonin-laden PLGA micropatterns were generated using the methods outlined in Figure 1. Briefly, PLGA (2.0 g; lactic/glycolic 1:1; M_w (molecular weight) 5000 and 10 000 Da, Sigma-Aldrich), or PLGA (2.0 g) and melatonin (5.0 mg; Wako, Japan) were dissolved in 20 mL of methylene chloride. The resulting PLGA solution (300 μL) or PLGA/melatonin composite solution (300 μL) was added onto a glass slide (1 cm × 1 cm), and then the Teflon stamp was covered on the glass slide under pressure (100 g/cm^2). The pressure was maintained for 12 h to allow complete evaporation of methylene chloride. The Teflon stamp was carefully removed from the glass slide to obtain the hardened PLGA micropattern on the glass slide. The PLGA micropattern on the chitosan film was fabricated using a similar route but replacing the glass slide with the chitosan film (drying 1% chitosan solution in an oven at 80 °C for 6 h). We observed the morphologies of the micropatterns using a microscope (CKX31, Olympus). PLGA flat film or melatonin-laden PLGA flat film was used as controls in cell experiments. We followed the following procedure for fabrication of the controls. The same concentration PLGA solution (2.0 g PLGA in 20 mL of methylene chloride) or PLGA/melatonin solution were poured onto a glass slide (1 cm × 1 cm), followed by covering of the Teflon stamp on the glass slide under pressure (100 g/

cm^2). The pressure was maintained for 12 h to allow complete evaporation of methylene chloride. In this work, the PLGA micropatterns with the groove widths of 100 and 50 μm were developed.

2.5. Degradation of PLGA Micropatterns. PGMs were weighed and then immersed in 20 mL of PBS solution (pH 7.2, Invitrogen) kept in separate plastic bottles. All the samples were incubated at 37 °C for 4 weeks. The samples were taken out every week, and surface water was removed. The dry weight of the samples was determined. Mass loss was calculated according to the following equation:

$$\text{mass loss}\ (\%) = [1 - (M_d/M_o)] \times 100$$

where M_d and M_o denote the dry and original weight of a PLGA micropattern, respectively.[39]

2.6. Cell Culture and Seeding. Human dermal fibroblasts were cultured in Dulbecco's modified Eagle's medium (DMEM) supplemented with 10% (v/v) fetal bovine serum (FBS), 100 units/mL penicillin, and 100 μg/mL streptomycin, and maintained in an incubator at 5% CO_2. The micropatterns were placed in cell culture dishes and sterilized under UV light for 30 min for each side. Two hundred microliters of cell suspension (3×10^5 cells/ml) was added on each micropattern and incubated in a humid atmosphere under 37 °C and 5% CO_2 in DMEM with 10% FBS. After a day of culture, the media were changed to remove nonadherent cells, and the media were subsequently changed every 3 days.

2.7. Cell Proliferation. Cell number was determined using cell counting kit-8 (Sigma-Aldrich) following the manufacturer's instruction. Briefly, after 1, 3, and 7 days of culture, the cell-laden PGM was washed with PBS three times, and then placed into a cell culture dish covered with 200 μL of DMEM and 20 μL of cell counting reagent. The dish was placed in a humidified incubator for 3 h, and the absorbance at 450 nm of the solution was measured using a plate reader (SynergyHT, BioTek). The cell number was achieved by comparing the value of absorbance with a standard curve.

2.8. Drug Release. The release of melatonin from PGMs was determined by suspending the drug-laden PGMs in PBS solution (pH value 7.2). The media from samples were collected periodically and replaced with the equal amount of PBS solution. The concentrations of released melatonin were measured at the maximum adsorption wavelength of melatonin (at 278 nm).[40]

2.9. Nuclei and F-Actin Staining. To visualize the size and morphology of fibroblasts on the PLGA micropatterns and melatonin-laden PGMs, cells were stained with DAPI (Invitrogen) for nuclei and TRITC-phalloidin (Invitrogen) for F-actin. Briefly, after 2 and 7 days of culture, samples were fixed with 1% formaldehyde for 15 min and 0.1% Triton X-100 (Sigma-Aldrinch) for 5 min. After washinh with PBS three times, the samples were stained with DAPI and TRITC-phalloidin for 30 min and then examined using a fluorescent microscope (Zeiss, Germany).

2.10. Quantification of Cellular Alignment. The shape of nuclei of cells was quantified by measuring their minimum and maximum diameter. The maximum diameter of nuclei is termed as their main axis. The angles between the main axis parallel with the grooves of PGM and the main axis of nuclei (considered as ellipses) was measured by NIH image software from the images of DAPI staining. The range of angles is from 0° to 90°, and a cell with the angle within less than 10° was considered as the alignment.[19]

2.11. Determination of Collagen. Collagen content was measured by the quantification of hydroxyproline. Briefly, fibroblasts cultured on the melatonin-laden PGM were digested and then added into a 4 M guanidine-HCl solution in 0.05 M sodium acetate. After centrifugation, the supernatant was discarded and then the residue was added into 5 mL of 6 M HCl and 2 mL of edible oil, and heated at 115 °C for 4 h. Afterward, the residue was treated in chloramine-T solution, perchloric acid solution, and paradime thylaminobenzaldehyde solution. The absorbance of the resulting solution at 560 nm was determined. Collagen quantification was calculated from a standard curve of hydroxyproline.[41]

2.12. Gene Expression. The cell-laden micropatterned PLGA was minced to approximately 1 cm × 1 cm piece used for RNA isolation. Minced scaffolds were homogenized in 1 mL of TRIzol reagent at room temperature for 30 min, and then the RNA isolation was conducted using TRIzol plus RNA purification kit (Invitrogen). Purified RNA was subjected to quantitative real-time PCR (qRT-PCR, Bio-Rad, MyiQ2 two color Real-Time PCR detection system) using SuperScript III Platinum SYBR green one-step qRT-PCR kit (Invitrogen) with custom-designed primers (Greiner Bio-One, Japan). The validated primer sequences of type I collagen are CCTGCGTGTACCCCACTCA (forward) and ACCAGACATGCC-TCTTGTCCTT (reverse). Data were analyzed using iCycler IQTM software. Gene expression was quantified by calculating $2^{\Delta Ct}$ values and $\Delta Ct = (Ct_{\beta\text{-actin}} - Ct_{\text{targetgene}})$.

2.13. Mechanical Properties. Mechanical properties of cell-laden PLGA micropatterns were measured using a universal testing machine (AG-X. Shimadzu, Japan) at a strain rate of 10 mm/min at room temperature (sample length and width are 1.0 cm).

2.14. Statistical Analysis. Six replicates were performed for every assay, and the results were expressed as means ± standard deviations. Statistical significance was determined by analysis of variance with $P < 0.05$.

3. RESULTS AND DISCUSSION

3.1. Generation of PLGA Micropatterns. Novel Teflon stamps were exploited to allow PLGA to be cast into a desired feature. The schemes for generating PLGA or drug-laden PLGA micropatterns using Teflon stamps are shown in Figure 1. Briefly, PLGA-methylene chloride solution or a drug-PLGA-methylene chloride composite solution was added onto a glass slide, and then was covered with a Teflon stamp under pressure. After complete evaporation of the organic solvent, the Teflon stamp was removed, and eventually the PLGA micropattern on the glass slide was obtained (Figure 2A).

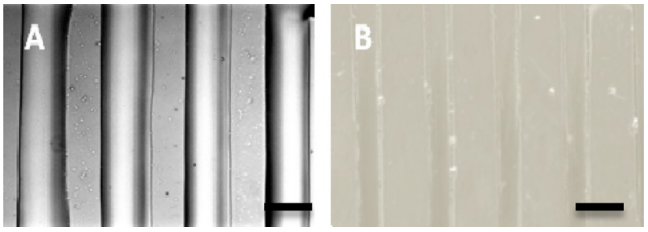

Figure 2. Microstructures of different PLGA micropatterns generated by Teflon stamps: PLGA micropatterns on glass slides (A); PLGA grooved micropattern on a chitosan film (B). (Scale bars: 100 μm.)

Besides using the glass slide as a substratum, PLGA micropatterns can be generated on the surface of various biomaterials such as chitosan film (Figure 2B). The micropattern on the surface of chitosan film exhibits a well-arranged morphology.

To confirm the superiorities of Teflon over PDMS for micropatterning PLGA (in its liquid state), two comparative experiments were performed. The first one is the capacity of Teflon and PDMS slides to resist harsh organic solvents. Here, we incubated the Teflon and PDMS flat slides into methylene chloride, respectively (Figure 3). After 3 h of incubation, the Teflon did not show any significant deformation, while the PDMS slide swelled with many obvious wrinkles on its surface. In addition, to compare the capacity of Teflon and PDMS on molecule adsorption, we incubated the Teflon and PDMS slides into 2% rhodamine solution and 2% fluoresceinisothiocyanato-dextran (FITC-Dex) for 3 h, respectively (Figure 4). The PDMS slides exhibited extremely significant adsorption of rhodamine (red color) and FITC-Dex (green color) when

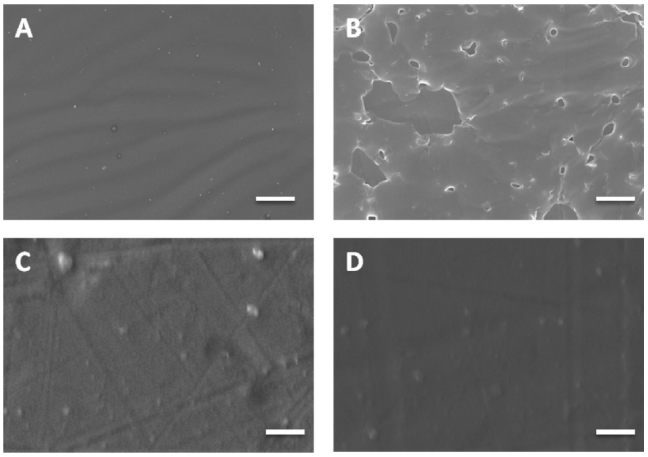

Figure 3. SEM images of original PDMS slide (A) and PDMS slide treated by methylene chloride for 3 h (B). Teflon slide (C) and Teflon slide treated by methylene chloride for 3 h (D). (Scale bars: 100 μm.)

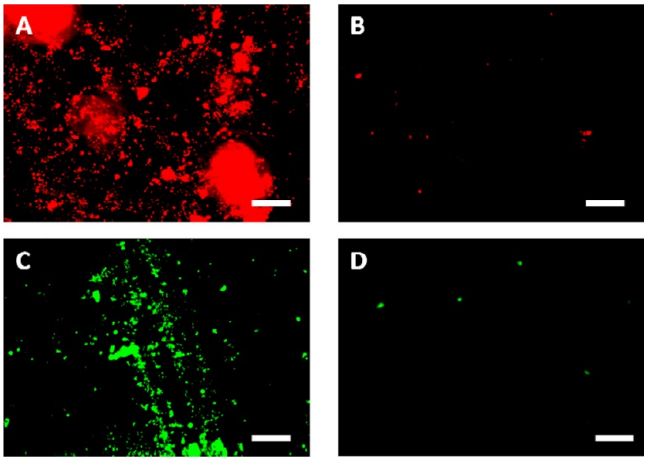

Figure 4. Fluorescent images of PDMS (A and C) and Teflon (B and D) slides incubated in 2% rhodamine solution (A and B) and 2% fluoresceinisothiocyanato-dextran solution (C and D) for 3 h. (Scale bars: 50 μm.)

compared with Teflon slides. We observed no fluorescence on the surface of Teflon slides.

The results shown in Figures 3 and 4 indicated that to pattern PLGA in its liquid phase into grooves, using Teflon as a stamp is mandatory. First, provided that a PDMS stamp was applied for generating the PLGA micropatterns, the microstructure of PDMS stamp will be seriously deformed and damaged by methylene chloride owing to the weak resistance of PDMS to harsh organic solvents (Figure 3). In contrast, Teflon stamp strongly resists to almost all the organic solvents (Figure 3).[32] Second, PDMS strongly adsorbs chemical/biological molecules on its surface while almost nothing sticks to Teflon surface (Figure 4).[32] Owing to this property, Teflon stamps will maximize the loading of drug/biomolecules into PLGA (Figure 4). Third, the generated PLGA micropattern can be easily released from the Teflon stamp after complete evaporation of the organic solvent because of the nonstick property of Teflon. In summary, Teflon stamps are more suitable for generating PLGA micropatterns or drug-laden PLGA micropatterns than PDMS stamps.

3.2. Degradable Properties. It is well known that the degradation time of PLGA varies from 1 month to several years (tailored by changing its molecular weight and the ratio of monomers).[42−44] Herein, PLGA with molecular weights (M_w) of 5000 and 10 000 Da was used for the generation of PGMs. The evaluation of PGM degradation was conducted in PBS solutions. The result reveals that PGMs with M_w of 5000 Da showed faster degradation than PGMs with M_w of 10 000 Da (Figure 5A). In the first week, both samples exhibited a slight

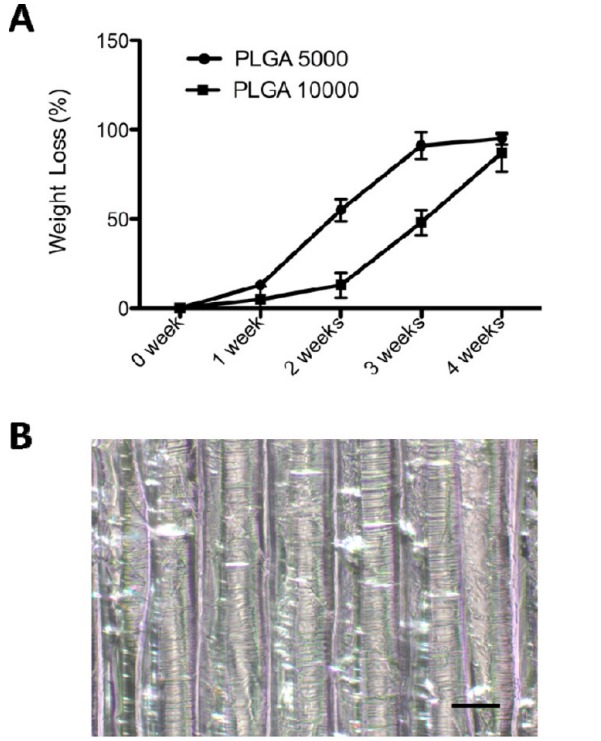

Figure 5. Degradation curves of PGMs (A) and the morphology of PGM (M_w: 10 000) after 2 weeks of incubation in PBS solution (B). (Scale bars: 100 μm.)

weight loss (less than 15%). Starting from the second week, PGMs with M_w of 5000 Da showed remarkable degradation; the weight loss of PGMs with M_w of 5000 Da was 3-fold and 2-fold higher than that of PGMs with M_w of 10 000 Da in the second week and the third week, respectively. During the third week, PGMs with M_w of 5000 Da almost completely degraded, while PGMs with M_w of 10 000 Da completely degraded in the fourth week. The morphology of PGMs with M_w of 10 000 Da incubated in PBS solution for 2 weeks is shown in Figure 5B. Although there were some wrinkles on the surface due to the surface degradation of PGMs, the ordered array still can be observed.

3.3. Cell Proliferation. To keep clear morphology of the micropattern for more than 1 week, PLGA with M_w of 10 000 Da was used for cell experiments. Cell numbers on PGMs after 1, 3, and 7 days of culture are shown in Figure 6A. Approximately 60 000 cells were seeded onto each PLGA grooved micropattern. After 1 day of culture, nonadherent cells were removed by changing the cell culture media. Around 30 000 cells were attached and adhered on the surface of the micropattern, so the cell adhesion efficiency of PGMs is approximately 50%. After 3 and 7 days of culture, cell proliferation was dramatically enhanced. The cell numbers at day 3 and day 7 were (51 200 ± 7700) and (81 100 ± 3600), respectively, which is around ∼1.5-fold and ∼2.5-fold higher

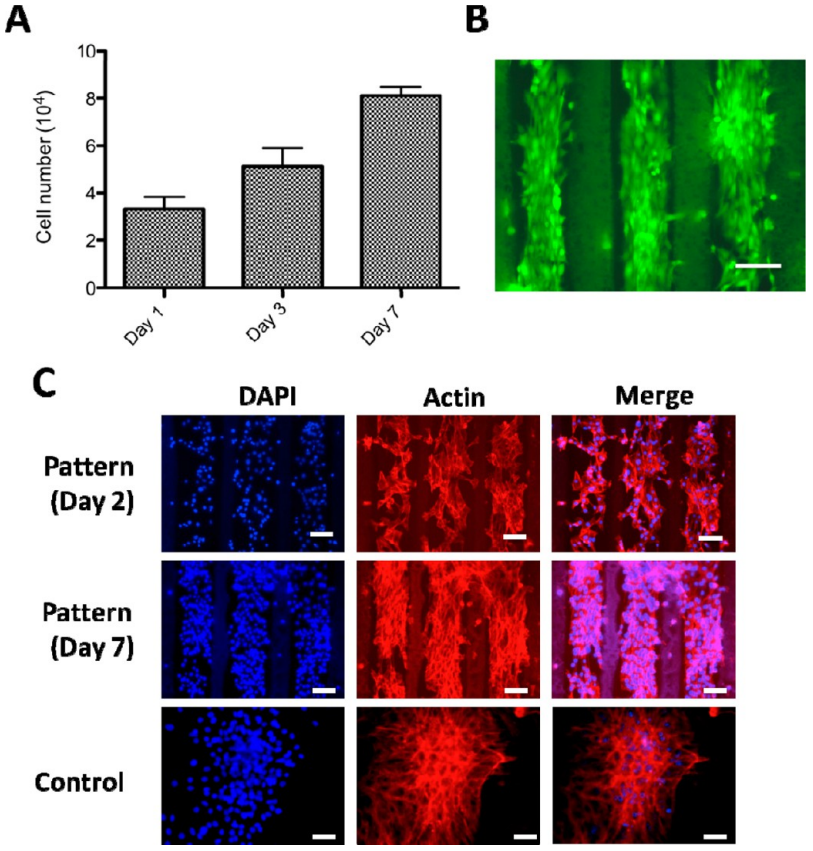

Figure 6. Cell number on PGMs after 1, 3, and 7 days of culture (A). Cell proliferation on PGMs after 7 days of culture examined by a fluorescent microscope (stained with live/dead assay) (B). Nuclei and F-actin staining of fibroblasts on PGMs after 2 and 7 days of culture. The PLGA film without pattern was used as control (C). (Scale bars, 200 μm).

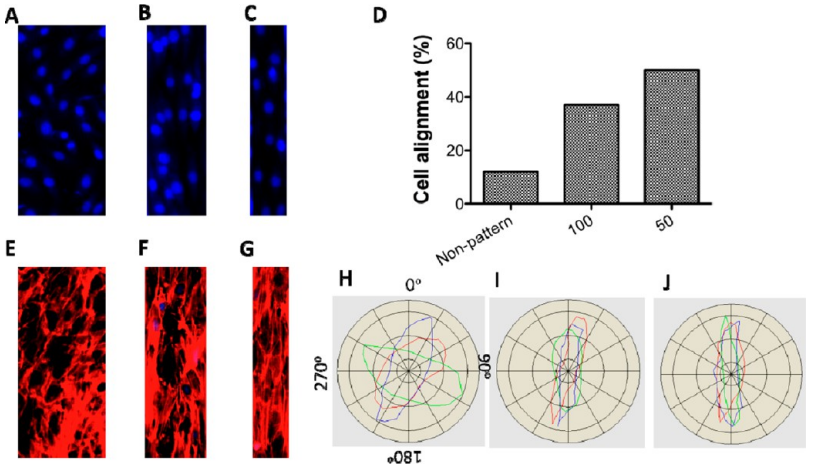

Figure 7. Images of aligned cell nuclei (A–C) and F-actin (E, F), and aligned cell nuclei counting (D) of fibroblasts on PGMs with groove with width of 100 μm (B, F) and 50 μm (C, G), and flat PLGA film (A, E), respectively. (I–H) Polar plots which reveal orientation distribution of F-actin of PGMs with groove with width of 100 μm, 50 μm, and flat PLGA film, respectively (each plot is an average of six replicates, and 90° and 270° represent the direction of groove).

than that at day 1 (33 200 ± 5200), indicating the outstanding support of PGMs for cell proliferation. The results were also verified by the live/dead assay (Figure 6B) after culturing for 7 days, in which live cells and dead cells fluoresce green and red, respectively. Almost no dead cells were observed on PGMs.

3.4. Directing Cellular Alignment. The grooved micropatterns can physically guide cells along the direction of the grooves and reorganize the cytoskeleton. Herein, dermal fibroblasts were seeded onto the PGMs, and the cell alignment was investigated. After 1 day of culture, fibroblasts seeded on the PGMs displayed actively self-organized behavior (Figures 6C and 7). Most of the fibroblasts were aggregated at the bottom of grooves instead of on the top of ridges of PGM. After 7 days of culture, the actin fibers of numerous cells preferentially oriented at the periphery of the channels and in the direction parallel with the grooves of PGM. In contrast,

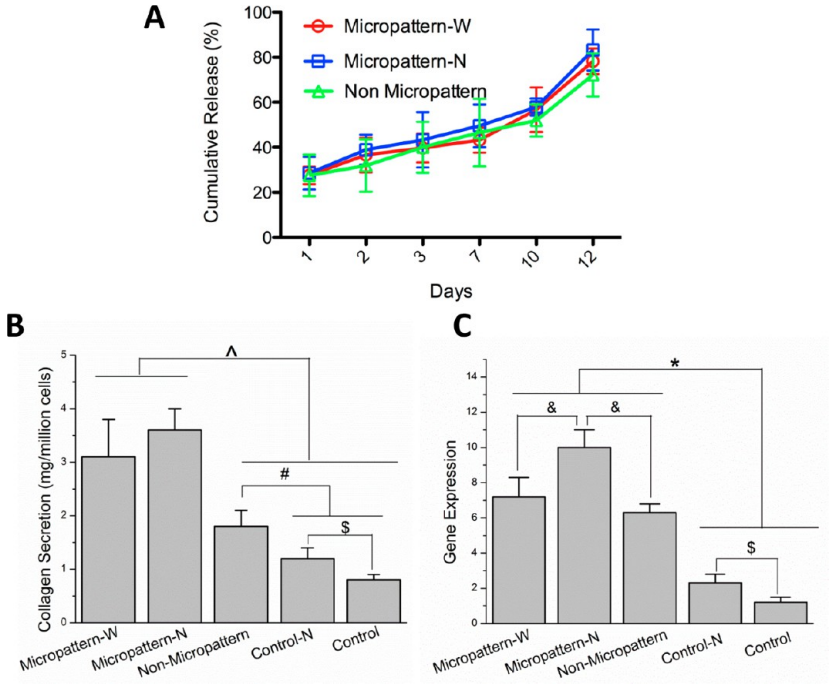

Figure 8. (A) Cumulative release profiles of melatonin from PGMs with groove wide of 100 μm (W) and 50 μm (N), and flat PLGA films. (B) Collagen secretion of fibroblasts on melatonin-laden PGMs with groove wide of 100 μm (W) and 50 μm (N), and flat melatonin-laden PLGA films after 7 days of culture, melatonin-free PGMs with groove wide of 50 μm (Control-N) and melatonin-free PLGA flat films (Control) were used as controls. Symbols ∧, ∗, #, &, and $ indicate statistical significance when compared with cells cultured on drug-laden PGMs, drug-laden PGMs and drug-laden PLGA flat film, drug-laden PLGA flat film, drug-laden PGM with groove width of 50 μm, and drug-free PLGA flat film, respectively ($p < 0.05$).

fibroblasts cultured on flat PLGA films did not exhibit observable tendency of alignment; most of the F-actin fibers were randomly distributed (Figure 7). Besides, the cellular alignment was quantitatively calculated by the nuclear alignment angles. The cell nuclei were stained with 4,6-diamidino-2-phenylindole (DAPI). The angle of the nuclear alignment less than 10 degree was considered to be well aligned. As shown in Figure 7D, approximately ∼50% cells grown on the PGMs with 50 μm grooves were aligned in contrast to ∼11% cells grown on the flat PLGA films and ∼38% cells grown on the PGMs with 100 μm grooves. The results clearly indicate that the cell alignment behavior can be effectively controlled by the topographical motifs of PGM.

3.5. Drug Release. It is well known that over 80% of the dry mass of tendon is collagen, and around 98% of the collagen portion is type I collagen. Therefore, for tendon repair, promoting the reconstruction of collagen is of great importance.[1,2] Melatonin, a hormone found in animals, has been used in nerve and bone tissue repair by significantly enhancing collagen secretion.[45,46] Here, we loaded melatonin into PGMs. Figure 8A shows the normalized release profiles of melatonin from PGMs with wide grooves (100 μm) and narrow grooves (50 μm). The release at each time point was normalized to the final drug loaded into PGMs. During the initial burst (the first 5 days), the drug release from PGMs was ∼50% of total drug loading amount. After 7 days, the total drug release from the micropatterns was more than 70%. Besides, drug-laden PGMs with wide grooves (100 μm), narrow grooves (50 μm), and flat PLGA film exhibited no significant differences on the release of melatonin.

3.6. Directing Protein and Gene Expression. Other than directing cell arrangement, melatonin-laden PGMs can also regulate the cellular phenotypes owing to continuous release of the loaded drug. In this study, dermal fibroblasts were used for evaluating potential tendon repair due to three main reasons. First, using autologous tenocytes may induce secondary tendon defect; second, dermal fibroblasts are easily derived and purchased. Importantly, dermal fibroblasts have been successfully used for repairing tendon in vivo.[47,48] As shown in Figure 8B and C, after 7 days of culture, the fibroblasts on melatonin-laden micropatterns exhibited higher-level protein expression of collagen and higher-level gene expression of type I collagen than those on the drug-free micropatterns. The enhanced extracellular matrix (collagen) deposition on the melatonin-laden PGMs is owing to the release of melatonin from PGMs.

It is well known that melatonin is a natural secretory product synthesized by the pineal gland.[49,50] It takes an important role in several biological functions. Nakade et al. reported that melatonin stimulated proliferation and collagen synthesis in human bone cells;[51] we achieved similar results in fibroblasts (Figure 7). The enhanced secretion of collagen, (approximately 65% of the dry mass of the tendon, and 90% of the collagen is type I collagen) which is the overwhelming majority protein in tendon confirmed the potential applications of the release of melatonin in tendon regeneration. Besides, the control of cell alignment can be used to regulate and enhance cell functions and phenotypes. Various studies have been performed to investigate the effect of cell alignment on cell behaviors. For example, aligned Schwann cells on a laminin micropattern showed higher potential on axonal regeneration.[52] An extracellular matrix pattern generated by microcontact printing on titanium effectively induced the alignment of osteoblasts for potential bone repair application.[53] In addition, the elongated and oriented morphology of endothelial cells corresponds with

a healthy phenotype.[54−56] Therefore, alignment of cells is of great importance for these tissues with a microscopically orientated appearance. Herein, the cells on the drug-laden micropatterns exhibited remarkable alignment, and the alignment of cells slightly promoted the expression of collagen (Figure 8). Besides, the chemical cue produced by the release of melatonin from PGMs enhanced the cell phenotypes. As shown in Figure 8, the melatonin-laden PGMs significantly promoted the expression of type I collagen and the secretion of collagen. Taken together, the melatonin-laden PLGA micropatterns not only induced the cell alignment mimicking the native morphology of tendon, but also promoted the cells to secrete extracellular matrix.

3.7. Mechanical Properties. We evaluated the mechanical properties of melatonin-laden PGMs, PGMs, flat PLGA films, and melatonin-laden flat films after 14 days of culture (Figure 9). Melatonin-laden PGM showed the highest tensile strength.

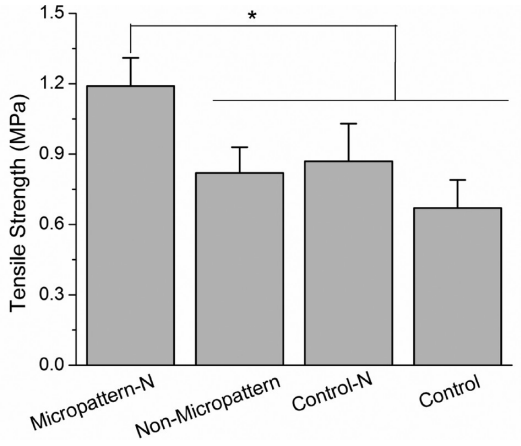

Figure 9. Mechanical property of melatonin-laden PGMs with groove wide of 50 μm (Micropattern-N) and flat melatonin-laden PLGA films (Non-micropattern). Melatonin-free PGMs with groove wide of 50 μm (Control-N) and melatonin-free PLGA flat films (Control) were used as controls. Asterisk (*) indicates statistical significance when compared with and flat melatonin-laden PLGA films (Non-micropattern), melatonin-free PGMs with groove wide of 50 μm (Control-N), and melatonin-free PLGA flat films (Control) ($p < 0.05$).

The tensile strength of PGMs is comparable to melatonin-laden flat films. Flat PLGA films exhibited the lowest tensile strength. The results suggested that the combination of grooved micropatterns (that promote the alignment cells and collagen) and melatonin release (that promotes the secretion of collagen) can significantly enhance mechanical property. Here, we used single layer cell laden films (two dimension); therefore, the tensile strength is significantly lower than that of natural tendon (a three-dimensional tissue). In the future, we will built multilayer films using the method developed in this study to investigate tendon regeneration in vivo.

4. CONCLUSION

In this study, a novel technique for generating biodegradable synthesized polymer micropatterns using Teflon stamps has been developed. Well-arranged PLGA grooved micropatterns and complex micropatterns were generated using Teflon stamps. The PLGA micropatterns exhibited regulatory, degradable properties. Melatonin-laden PLGA grooved micropatterns showed excellent biocompatibility as well as the property to direct cell behavior, indicating the great potential on tendon restoration. We conclude that the developed drug-laden micropatterns using Teflon stamp not only provide a conceptual framework for tissue regeneration that combine the topological cue and chemical cue, but also propose a facile and novel method to construct a micropatterned model using synthetic polymers.

AUTHOR INFORMATION

Corresponding Authors

*(X.S.) E-mail: shiixuetao@gmail.com.

*(H.W.) E-mail: chhkwu@ust.hk. Tel: +81-22-217-5998. Fax: +81-22-217-5997.

Notes

The authors declare no competing financial interest.

ACKNOWLEDGMENTS

This work was supported by WPI-Initiative funding from Japan Society for Promotion of Science and Ministry of Education, Culture, Sports, Science and Technology, Japan. H.K.W. acknowledges the support from Hong Kong RGC (GRF 604712 and GRF 605210).

REFERENCES

(1) Liu, Y.; Ramanath, H. S.; Wang, D.-A. *Trends Biotechnol.* **2008**, *26*, 201−209.
(2) Saltzma, C. L.; Tearse, D. S. *J. Am. Acad. Orthop. Surg.* **1998**, *6*, 316−325.
(3) Fan, J.; Varshney, R. R.; Ren, L.; Cai, D.; Wang, D.-A. *Tissue Eng.* **2009**, *15*, 75−86.
(4) Wang, J. H. C. *J. Biomech.* **2006**, *39*, 1563−1582.
(5) Huang, D.; Balian, G.; Chhabra, A. *J. Hand Surg.* **2006**, *31*, 693−704.
(6) Sahoo, S.; Ouyang, H.; James, J. C.; Goh, T.; Tay, E.; Toh, S. L. *Tissue Eng.* **2006**, *12*, 91−99.
(7) Pennisi, E. *Science* **2002**, *295*, 1011.
(8) Pins, G. D.; Christiansen, D. L.; Patel, R.; Silver, H. F. *Biophys. J.* **1997**, *73*, 2164−2172.
(9) Jacobs, H. O.; Whitesides, G. M. *Science* **2001**, *291*, 1763−1766.
(10) Whitesides, G. M.; Ostuni, E. S.; Takayama, S.; Jiang, X.; Ingber, D. E. *Ann. Rev. Biomed. Eng.* **2001**, *3*, 335−373.
(11) Whitesides, G. M.; Love, J. C. *Sci. Am.* **2001**, *285*, 32−41.
(12) Jiang, X.; Ferrigno, R.; Mrksich, M.; Whitesides, G. M. *J. Am. Chem. Soc.* **2003**, *125*, 2366−2367.
(13) Paul, K. E.; Prentiss, M. G.; Whitesides, G. M. *Adv. Funct. Mater.* **2003**, *13*, 259−263.
(14) Wu, H. K.; Odom, T. W.; Chiu, D. T.; Whitesides, G. M. *J. Am. Chem. Soc.* **2003**, *125*, 554−559.
(15) Mayer, M.; Yang, J.; Gitlin, I.; Gracias, D. H.; Whitesides, G. M. *Proteomics* **2004**, *4*, 2366−2376.
(16) Bajaj, P.; Reddy, B., Jr.; Millet, L.; Wei, C.; Zorlutuna, P.; Bao, G.; Bashir, R. *Integr. Biol.* **2011**, *3*, 897−909.
(17) Cimetta, E.; Pizzato, S.; Bollini, S.; Serena, E.; De Coppi, P.; Elvassore, N. *Biomed. Microdevices* **2009**, *11*, 389−400.
(18) Shi, X.; Chen, S.; Zhou, J.; Yu, H.; Li, L.; Wu, H. *Adv. Funct. Mater.* **2012**, *22*, 3799−3807.
(19) Yoon, S.-H.; Kim, Y. K.; Han, E. D.; Seo, Y.-H.; Kim, B. H.; Mofrad, M. R. K. *Lab Chip* **2012**, *12*, 2391−2402.
(20) Aw, M. S.; Addai-Mensah, J.; Losic, D. *Chem. Commun.* **2012**, *48*, 3348−3350.
(21) Shi, X.; Wang, Y.; Ren, L.; Gong, Y.; Wang, D.-A. *Pharm. Res.* **2009**, *26*, 422−430.
(22) Park, K. M.; Jun, I.; Joung, Y. K.; Shin, H.; Park, K. D. *Soft Matter* **2011**, *7*, 986−992.
(23) Shi, X.; Wang, Y.; Varshney, R. R.; Ren, L.; Gong, Y.; Wang, D.-A. *Eur. J. Pharm. Sci.* **2010**, *29*, 59−67.

(24) Huang, W.; Wang, Y.; Ren, L.; Du, C.; Shi, X. *Mater. Sci. Eng. C* **2009**, *29*, 2221−2225.
(25) Wang, Y.; Shi, X.; Ren, L.; Wang, C.; Wang, D.-A. *Mater. Sci. Eng. C* **2009**, *29*, 2502−2507.
(26) Shi, X.; Su, K.; Varshney, R. R.; Wang, Y.; Wang, D. A. *Pharm. Res.* **2011**, *28*, 1224−1228.
(27) Shi, X.; Wang, Y.; Ren, L.; Lai, C.; Gong, Y.; Wang, D. A. *J. Biomed. Mater. Res. A* **2010**, *92A*, 963−972.
(28) Shi, X.; Li, R.; Tian, M.; Yu, J.; Huang, W.; Du, C.; Wang, D. A.; Wang, Y. J. *J. Mater. Chem.* **2010**, *20*, 9140−9148.
(29) Shi, X.; Wang, Y.; Varshney, R. R.; Ren, L.; Zhang, F.; Wang, D. A. *Biomaterials* **2009**, *30*, 3996−4005.
(30) Sahay, R.; Kumar, S.; Sridhar, R.; Sundaramurthy, J.; Venugopal, J.; Mhaisalkar, S. G.; Ramakrishna, S. *J. Mater. Chem.* **2012**, *22*, 12953−12971.
(31) Kobe, S.; Limacher, M.; Gobaa, S.; Laroche, T.; Lutolf, M. P. *Langmuir* **2009**, *25*, 8774−8779.
(32) Ren, K.; Dai, W.; Zhou, J.; Su, J.; Wu, H. *Proc. Natl. Acad. Sci. U.S.A.* **2011**, *108*, 8162−8166.
(33) Dai, W.; Zheng, Y.; Lou, K. Q.; Wu, H. *Biomicrofluidics* **2010**, *4*, 024101.
(34) Roth, J. A.; Kim, B.-J.; Lin, W.-L.; Cho, M.-I. *J. Biol. Chem.* **1999**, *274*, 22041−22047.
(35) Ostrovidov, S.; Sakai, Y.; Fujii, T. *Biomed. Microdevices* **2011**, *13*, 847−864.
(36) Mizuno, J.; Ostrovidov, S.; Sakai, Y.; Fujii, T.; Nakamura, H.; Inui, H. *Fertil. Steril.* **2007**, *88*, S101.
(37) Shi, X.; Zhou, J.; Zhao, Y.; Li, L.; Wu, H. *Adv. Healthcare Mater.* **2013**, *2*, 846−853.
(38) Wu, H.; Wheeler, A. R.; Zare, R. N. *Proc. Natl. Acad. Sci. U.S.A.* **2004**, *101*, 12809−12813.
(39) Shi, X.; Wang, Y.; Ren, L.; Huang, W.; Wang, D. A. *Int. J. Pharm.* **2009**, *373*, 85−92.
(40) Shi, X.; Wang, Y.; Ren, L.; Zhao, N.; Gong, Y.; Wang, D. A. *Acta Biomater.* **2009**, *5*, 1697−1707.
(41) Surmeian, M.; Aboul-Enein, H. Y. *Analyt. Lett* **1998**, *31*, 1731−1741.
(42) Kopeček, J. *Biomaterials* **2007**, *28*, 5185−5192.
(43) Anderson, J. M.; Shive, M. S. *Adv. Drug Delivery Rev.* **1997**, *28*, 5−24.
(44) Sinha, V. R.; Trehan, A. *J. Control. Release* **2003**, *90*, 261−280.
(45) Nakade, O.; Koyama, H.; Ariji, H.; Yajima, A.; Kaku, T. *J. Pineal Res.* **2007**, *27*, 106−110.
(46) Bekir, A.; Ibrahim, E.; Mustafa, T.; Hakan, B.; Mehmet, B.; Sadrettin, P. *J. Surg. Res.* **2011**, *166*, 330−336.
(47) Liu, W.; Chen, B.; Deng, D.; Xu, F.; Cui, L.; Cao, Y. *Tissue Eng.* **2006**, *12*, 775−788.
(48) Deng, D.; Liu, W.; Xu, F.; Yang, Y.; Zhou, G.; Zhang, W. J.; Cui, L.; Cao, Y. *Biomaterials* **2009**, *30*, 6724−6730.
(49) Cutando, A.; López-Valverde, A.; Arias-Santiago, S.; DE Vicente, J.; De Diego, R. G. *Anticancer Res.* **2012**, *32*, 2747−2753.
(50) Kitagawa, A.; Ohta, Y.; Ohashi, K. *J. Pineal Res.* **2012**, *52*, 403−413.
(51) Nakade, O.; Koyama, H.; Ariji, H.; Yajima, A.; Kaku, T. *J. Pineal Res.* **1999**, *27*, 106−110.
(52) Thomson, D. M.; Buettner, H. M. *Tissue Eng.* **2001**, *7*, 247−266.
(53) Zhang, J. T.; Nie, J.; Mühlstädt, M.; Gallagher, H.; Pullig, O.; Jandt, K. D. *Adv. Funct. Mater.* **2011**, *21*, 4079−4087.
(54) Moretti, M.; Prina-Mello, A.; Reid, A. J.; Barron, V.; Prendergast, P. J. *J. Mater. Sci.: Mater. Med.* **2004**, *15*, 1159−1164.
(55) Malek, A. M.; Izumo, S. *J. Cell Sci.* **1996**, *109*, 713−726.
(56) Bouta, E. M.; McCarthy, C. M.; Keim, A.; Wang, H. B.; Gilbert, R. J.; Goldman, J. *Acta Biomater.* **2011**, *7*, 1104−1113.